12-14-2017

Erosion in Extruder Flows: Analytical and Numerical Study

Miron Kaufman
Cleveland State University, m.kaufman@csuohio.edu

Petru S. Fodor
Cleveland State University, p.fodor@csuohio.edu

Erosion in extruder flows: Analytical and numerical study

Cite as: AIP Conference Proceedings **1914**, 080003 (2017); https://doi.org/10.1063/1.5016743
Published Online: 15 December 2017

Miron Kaufman, and Petru S. Fodor

Erosion in Extruder Flows: Analytical and Numerical Study

Miron Kaufman* and Petru S. Fodor

Department of Physics, Cleveland State University, 2121 Euclid Avenue, Cleveland, OH 44115, USA

m.kaufman@csuohio.edu

Abstract. We consider the erosion of particles (e.g. carbonblack agglomerates) advected by the polymeric flow in a single screw extruder. We assume a particle to be made of primary fragments bound together. In the erosion process a primary fragment breaks out of a given particle. Particles disperse because of the shear stresses imparted by the fluid. The time evolution of the numbers of particles of different sizes is described by the Bateman coupled differential equations developed a century ago to model radioactivity. Using the particle size distribution we compute an entropic fragmentation index which varies from 0 for a monodisperse system to 1 for an extreme poly-disperse system. The time dependence of the index exhibits a maximum at some intermediate time as the system starts monodisperse (large size particle) and evolves through a poly-disperse regime at intermediate times to a monodisperse (small size particle) at late times..

Keywords: Single-Screw Extruder; Particle Tracing; Particle Fragmentation; Erosion.
PACS: 47.15.Rq; 47.85.md; 47.55.Kf.

INTRODUCTION

We extend and adapt to polymer processes a model that we proposed [1] to describe erosion in microchannel flows. A model of erosion and rupture of agglomerates carried by melt in an extruder was analyzed with Monte-Carlo simulation [2]. The particles are advected by an incompressible flow and erode because of the shear stresses imparted by the fluid. A particle with a larger surface area is further assumed to be more likely to erode than a particle with a smaller surface area. The extruder is modelled using Tadmor's unwound channel model [3]. We consider the creeping flow in an infinitely long extruder driven by the pressure gradient and drag along the extruder axis. We demonstrate that under those circumstances there is an analytic solution to the fragmentation equations, based on the solution of the Bateman equations [4] of nuclear physics. This quantification of fragmentation of particles advected by a fluid in an extruder is important for the design and optimization of this polymer technology. To evaluate the level of fragmentation we use the Shannon-information entropy [5] which was applied [6] also to quantify distributive and component mixing.

FRAGMENTATION MODEL

We model the particles advected by the extruder flow as being made of s primary fragments bound together. An erosion event is the breakage of a particle of size s into a primary fragment and a particle of size $s-1$. We define an index m to label a certain size: $s(m) = M - m + 1$, where M is the size of the largest particle, and $m = 1, 2, \ldots, M$. The particles are advected by the laminar flow and erode due to the flow shearing. The process of erosion is assumed to be a Poisson random process, in which any aggregate particle erodes during a time interval with a probability that is proportional with the time interval. The rate of change of the mean number of particles of type m is equal to the difference between the mean number of particles of type $m-1$ and type m, respectively, that erode per unit time. The numbers of aggregate particles of type m, each such particle containing $M - m + 1$ primary particles, satisfy a set of coupled differential equations:

$$\frac{dN_{m,\vec{r}(t)}(t)}{dt} = -\lambda_{m,\vec{r}(t)}(t) N_{m,\vec{r}(t)}(t) + \lambda_{m-1,\vec{r}(t)}(t) N_{m-1,\vec{r}(t)}(t) \tag{1}$$

where $\lambda_{0,\vec{r}(t)}(t) = \lambda_{M,\vec{r}(t)}(t) = 0$ and $m = 1, 2, \ldots M$. In Eq. (1) λ stands for the erosion probability rate.

Particles disperse because of the shear stresses imparted by the fluid. We assume the erosion probability rate λ is proportional to the largest component of the shear stress tensor σ and inversely proportional to the cohesive stress.

Proceedings of PPS-32
AIP Conf. Proc. 1914, 080003-1–080003-5; https://doi.org/10.1063/1.5016743
Published by AIP Publishing. 978-0-7354-1606-2/$30.00

We further assume that a particle with a larger surface area has a higher chance to erode than a particle with a smaller surface area. Particles of the smallest size, i.e. $m = 1$, do not decay. Hence we postulate that for a particle of size s, the erosion probability rate λ is proportional to $(s - 1)^{2/3}$. Thus the erosion rate of a particle of type m is:

$$\lambda_{m,\vec{r}(t)} = \frac{(s(m)-1)^{2/3} \max(|\sigma_{x,y}|,|\sigma_{y,z}|,|\sigma_{z,x}|)}{\tau\sigma_0} \tag{2}$$

where τ is a characteristic time and σ_0 is the cohesive stress of the particle.

We compute the shear stress tensor by solving the Navier-Stokes and continuity equations for incompressible Newtonian fluids, in the limit of zero Reynolds number and assuming that steady state has been achieved. The channel is a parallelepiped with a rectangular cross-section. Since the axial length is much longer than the cross-sectional size, we assume an infinitely long rectangular channel. It follows that the three components of the velocity depend only on transversal coordinates: **V**(X,Y). Furthermore since the walls are fixed or move in z direction there is no drag to induce fluid circulation in the xy plane: $V_x = V_y = 0$. The solution for the velocity along z direction is given in Ref. 3:

$$\begin{aligned} \frac{V_z}{V_B} &= \frac{4}{\pi}\sum_{n=1}^{\infty}\frac{\sinh((2n+1)\pi y/w)}{(2n+1)\sinh((2n+1)\pi/w)}\sin\left((2n+1)\pi x/w\right)+ \\ &+\frac{H^2}{2\eta V_B}\frac{\partial p}{\partial z}[y^2-y+\frac{8}{\pi^3}\sum_{n=1}^{\infty}\frac{\cosh\left((2n+1)\pi(x-w/2)\right)}{(2n+1)^3\cosh\left((2n+1)\pi w/2\right)}\sin\left((2n+1)\pi y\right)] \end{aligned} \tag{3}$$

where V_B is the wall velocity, $x = X/H$, $y = Y/H$ and $w = W/H$. The shear stress tensor components, needed to compute the erosion rates from Eq. (2), are:

$$\begin{aligned} \sigma_{x,z} &= \sigma_{z,x} = \eta\frac{\partial V_z}{\partial X} \\ \sigma_{y,z} &= \sigma_{z,y} = \eta\frac{\partial V_z}{\partial Y} \\ \sigma_{x,y} &= \sigma_{y,x} = 0 \end{aligned} \tag{4}$$

Depending on the flow characteristics the erosion probability rates λ may depend on time. However in the current work, where we study the creeping flow driven by a pressure gradient and drag along the axis in a long extruder, the shear stress does not change along the flow line and thus the probability rates λ are time constants. A flow line is specified by giving the transversal coordinates x and y. Equations (1) are then identical to the Bateman equations [4] used in nuclear physics to model radioactive series. Under the initial conditions:

$$N_{m,x,y}(0) = 0 \text{ where m = 2, 3,…, M} \tag{5}$$

the solutions to the set of differential equations (1) is:

$$N_{n,x,y}(t) = N_{1,x,y}(0)\sum_{i=1}^{n} c(n,i,x,y)e^{-\lambda_{i,x,y}t} \text{ for n = 1, 2,…,M} \tag{6}$$

where:

$$c(m,j,x,y) = 1 \text{ if m = j = 1} \tag{7}$$

$$c(m,j,x,y) = \frac{\prod_{i=1}^{m-1} \lambda_{(i,x,y)}}{\prod_{i=1, i\neq j}^{m} (\lambda_{(i,x,y)} - \lambda_{(j,x,y)})} \quad \text{if } 1 \leq j \leq m \tag{8}$$

Using Eqs. (5) – (8), one gets a set of nontrivial identities that have been used [7] to derive sum rules relating light scattering intensities from the different coexisting phases close to a multicritical point in liquid mixtures.

To quantify the fragmentation process we define a measure based on the Shannon entropy:

$$S_{x,y}(t) = -\sum_{m=1}^{M} \frac{N_{m,x,y}(t)}{N_{x,y}} \ln(\frac{N_{m,x,y}(t)}{N_{x,y}}) \tag{9}$$

where:

$$N_{x,y} = \sum_{m=1}^{M} N_{m,x,y}(t) \tag{10}$$

S as defined in Eq. (9) is a positive quantity with a maximum possible value of $ln(M)$ achieved when all populations are equal to each other. We define the fragmentation index $S/ln(M)$ which is zero when one population fraction is 1 and the others are zero, i.e. monodisperse system, and it is 1 when all populations are equal in size; i.e. extremely poly-disperse system.

RESULTS

There are two dimensionless numbers associated with this problem, The first number $\mathcal{N}_1$ compares the drag time H/V_B to the fragmentation time $1/\lambda \sim \tau\sigma_0 H/(\eta V_B)$. It is equal to:

$$\mathcal{N}_1 = \frac{\eta}{\tau\sigma_0} \tag{11}$$

When $\mathcal{N}_1 << 1$ the fragmentation process is weak as the agglomerate particles are resilient. If $\mathcal{N}_1 >> 1$ the agglomerates are very brittle. The numerical results below are obtained for the intermediate regime where $\mathcal{N}_1 = 1$.

The second number $\mathcal{N}_2$ compares the effect of the pressure gradient on the flow speed to that of the wall drag:

$$\mathcal{N}_2 = -\frac{H^2}{2\eta V_B}\frac{\partial p}{\partial z} \tag{12}$$

We model the fragmentation process for the following three choices: (i) pure pressure driven flow: $\mathcal{N}_2 = \infty$; (ii) pure drag flow: $\mathcal{N}_2 = 0$; and (iii) mixed pressure and drag flow $\mathcal{N}_2 = 1$. All results of this section are presented using dimensionless quantities. Distances are expressed in units of the height of the rectangular cross-section size H and time is expressed in units of H/V_B. We consider an aspect ratio $w = W/H = 3$ and the size of the largest particle to be $M = 21$.

In Figure 1 we show the time evolution of the number of particles of types 1, 5, 10, 15, and 21, respectively for the flow line defined by $x = 0.2$, $y = 0.3$. $N_{1,x,y}$ drops monotonically from its initial value and $N_{5,x,y}$ builds up from zero (initial value) goes through a peak at $t = 0.2$. Similar dependence is exhibited by the other population numbers with peaks occurring at later times. The knowledge of the time evolution in the number of particles of different sizes is used to characterize the size dispersion of the system and its time evolution based on the entropic fragmentation index given by equation (9).

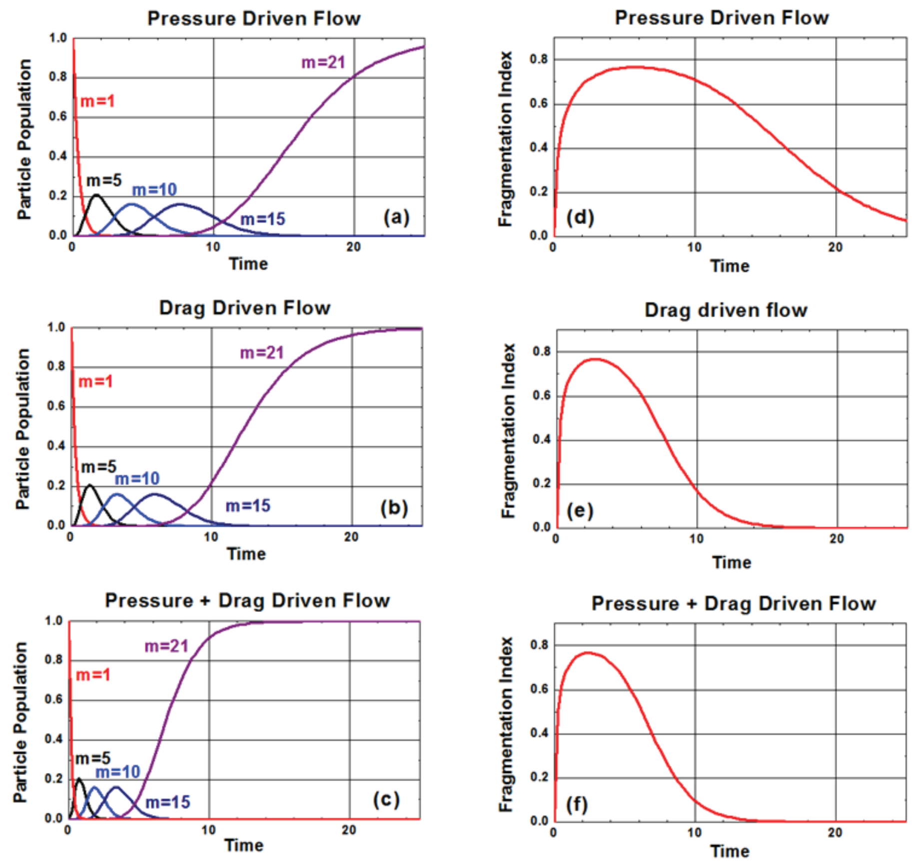

FIGURE 1. (a), (b), and (c) Time evolution of the population fractions of the different type of driven flows considered; (d), (e), and (f) The corresponding entropic fragmentation index vs. time.

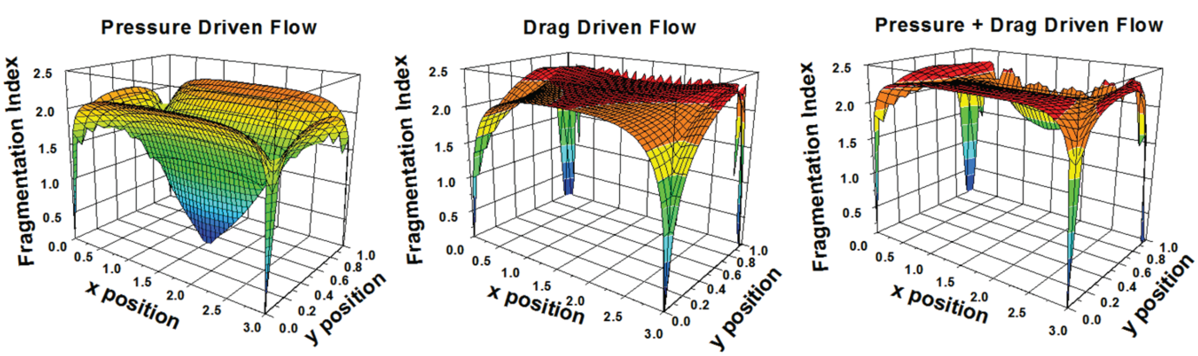

FIGURE 2. Position dependence of the fragmentation index at $t = 1$.

As observed in Figure 1 the index $S/ln(M)$ varies from 0 for a monodisperse system to 1 for an extremely polydisperse system. The time dependence of the index exhibits a maximum at some intermediate time as the system starts monodisperse (large size particles) and evolves through a polydisperse regime at intermediate times to a monodisperse (but with small size particles) at late times. Note that the maximum value of the fragmentation index is less than unity. This is due to the fact that not all size particles are present.

Since the fragmentation entropic index depends on the flow line, we show in Figure 2 the dependence of the entropy ($0 < S < ln21$) on x and y at t = 1. We assume for initial condition a uniform distribution in the xy plane of particles of largest size ($M = 21$) only. Note the system is monodisperse at the corners and in the center of the cross-section. This result is explained by the fact that at these points the shear stress is zero.

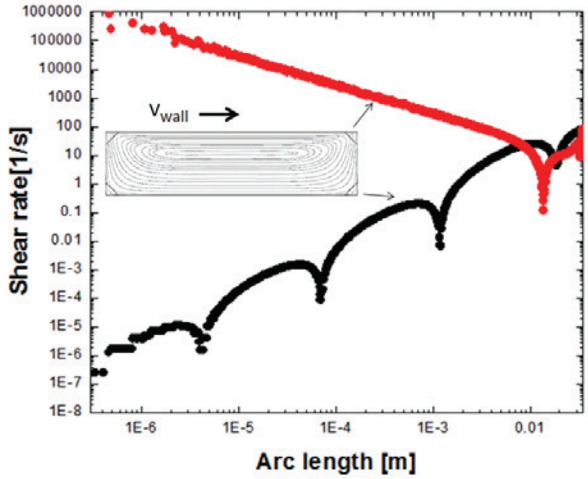

FIGURE 3. Shear rates away from the singular points represented by the extruder corners. The top corner is defined by a moving and a stationary wall, while for the bottom corner both walls are stationary.

SUMMARY

We have presented a model for fragmentation of particles advected by laminar flows in extruders. We have also introduced an index of fragmentation based on the information entropy that is useful for various optimization tasks. For instance we can determine the minimum time needed to reach a desired level of fragmentation, based on the time evolution of this fragmentation index.

Due to certain simplifying assumptions, such as zero Reynolds number, we were able to solve the model analytically by employing the Bateman equations of nuclear physics. It is desirable to improve the model by relaxing some of those assumptions. In particular in an extruder modeled using the Tadmor's unwound channel model [3] the wall of the cavity moves diagonally and thus drag forces are present in the cross section of the system. This leads to the formation of complicated flow structures such as Moffatt eddies [8], associated with singularities imposed by the boundary conditions at the corners. As seen in Fig. 3, numerical simulations of these flows indicate that the shear rates for these systems are quite complex and will affect both the fragmentation rates as well as the distribution of fragments within the volume of the extruder. Given the complexity of these systems a combination of numerical and analytical methods is warranted for tackling the problem [9, 10]. Under this approach, an analytical solution, as described above can be used to obtain the longitudinal velocity field (in the limit of zero Reynolds number). This allows us to devote all the computational resources solely for a detailed numerical solution of the transversal velocity field. The combined 3D solution for the flow field can then be used with the above described model to characterize the fragmentation process within the extruder type system.

REFERENCES

1. M. Kaufman, *Nanoscale and Microscale Thermophysical Engineering* **11**, 129–136 (2007).
2. N. Domingues, M. Camesasca, M. Kaufman, I. Manas-Zloczower, A. Gaspar-Cunha, J. A. Covas, *International Polymer Processing* **XXV**, 251-257 (2010).
3. Z. Tadmor and C.G. Gogos, "Chapter 6 – Pressurization and Pumping," in *Principles of Polymer Processing, 2nd edition*, Wiley-Interscience, Hoboken, New Jersey, 2006.
4. H. Bateman, *Proc. Cambridge Philos. Soc*. **15**, 423-427 (1910).
5. C. E. Shannon and W. Weaver, in *The Mathematical Theory of Communication,* University of Illinois Press, Urbana, Illinois, 1949.
6. K. Alemaskin, I. Manas-Zloczower, and M. Kaufman, *Polymer Engineering and Science* **45**, 1011-1020 (2005).
7. M. Kaufman and M. Ma, *Phys. Rev. A* **35**, 2369-2372 (1987).
8. H.K. Moffatt, *J. Fluid Mech*. **18**, 1 – 18 (1963).
9. M. Kaufman and P.S. Fodor, *Physica A* **389**, 2951-2955 (2010).
10. P. S. Fodor, M Kaufman, *AIP Conf. Proc.* **1664**, 050010 (2015).